A NEW RF STRUCTURE FOR INTERMEDIATE-VELOCITY PARTICLES[*]

James H. Billen, Frank L. Krawczyk, Richard L. Wood, and Lloyd M. Young
Los Alamos National Laboratory
MS H817, Los Alamos, NM 87545, USA

Abstract

This paper describes an rf structure with high shunt impedance and good field stability for particle velocities $0.1 \leq \beta \leq 0.5$. Traditionally, the drift-tube linac (DTL) has been the structure of choice for this velocity range. The new structure, called a coupled-cavity drift-tube linac (CCDTL), combines features of the Alvarez DTL and the π-mode coupled-cavity linac (CCL). Each accelerating cavity is a two-cell, 0-mode DTL. The center-to-center distance between gaps is $\beta\lambda$. Adjacent accelerating cavities have oppositely directed electric fields, alternating in phase by 180°. The chain of cavities operates in a $\pi/2$ structure mode so the coupling cavities are nominally unexcited. We will discuss 2-D and 3-D electromagnetic code calculations, and some initial measurements on a low-power model of a CCDTL. We will compare shunt impedance calculations for DTL, CCL, and CCDTL structures. The CCDTL has potential application for a wide range of ion linacs. For example, high-intensity proton linacs could use the CCDTL instead of a DTL up to an energy of about 200 MeV. Another example is a stand-alone, low-duty, low-current, very high gradient, proton, cancer therapy machine. The advantage for this application would be a saving in the cost of the machine because the linac would be short.

The RF Structure

Figure 1 is a sketch of a CCDTL section for velocity $\beta = 0.314$, which corresponds to 50-MeV protons. Each accelerating cavity is a two-cell DTL operated in the TM_{010}-like mode, which means that the accelerating field points in the same direction in both gaps at a given instant of time. Arrows on the beam axis show the electric field direction. The center-to-center distance between gaps is $\beta\lambda$, where λ is the free-space wavelength of the resonant mode. Adjacent accelerating cavities have oppositely directed electric fields, alternating in phase by 180 degrees or π radians. The chain of cavities operates in a $\pi/2$ structure mode so the coupling cavities are nominally unexcited. The center of the first gap in a cavity is $\beta\lambda/2$ past the center of the last gap in the previous cavity. Thus, the total length of each accelerating cavity is $3\beta\lambda/2$. This scheme ensures that a particle always encounters an accelerating field in every gap. Figure 1 shows a side-coupled structure, but one also might use on-axis coupling or any other arrangement commonly applied to ordinary CCLs. The stem on each drift tube is merely pictorial. Its best orientation would be 90° from the coupling slots to minimize field asymmetries near the slots. To facilitate cooling or to improve the mechanical stability, one might use two stems.
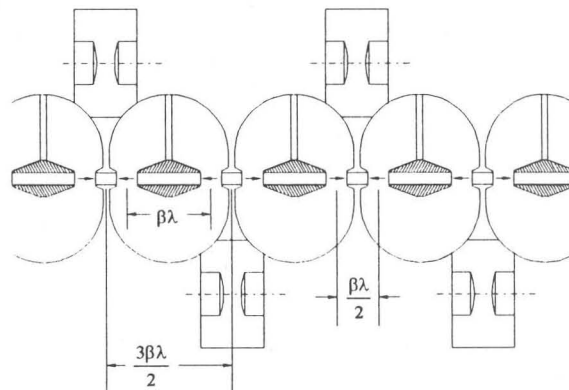
Figure 1. A coupled-cavity drift-tube linac structure for $\beta = 0.314$ with a single drift tube in each cavity.
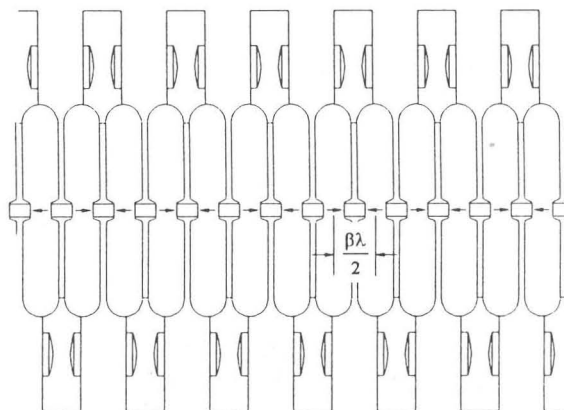

Figure 2. A coupled-cavity linac structure for the same particle velocity as the CCDTL in Fig. 1.

A proton energy of 50 MeV is well below the energy for which one would build a CCL. For example, the CCL at the Los Alamos Meson Physics Facility (LAMPF) starts at 100 MeV.[1] The design of the CCL for the former supercollider (SSC) started at 70 MeV.[2] Figure 2 shows a section of $\beta = 0.314$ CCL. Compare this hypothetical structure to the CCDTL structure in Figure 1, which corresponds to the same particle velocity. The large number of walls per unit length gives this CCL a very poor efficiency as measured by the shunt impedance per unit length. It also has three times the number of coupling cavities per unit length as the CCDTL.

Accelerating Cavity Design

Figure 3 shows plots from the 2-D code SUPERFISH of electric-field lines in cylindrically symmetric half cavities. The figure actually shows contours of constant rH, with more contours near H = 0 to better show the field direction in the bore. (Line density is not related to field strength.) The shape of the cavity wall is similar to that of an ordinary CCL cell designed for higher β, except that the space between the wall noses is large enough either for two gaps and a drift tube or three gaps and two drift tubes. The cavity has a large outer corner radius to reduce the surface to volume ratio. The gap between noses is approximately βλ/4 resulting in a reasonably large transit-time factor. Drift tubes in the CCDTL would probably not contain magnets so fabrication of the structure would use conventional CCL brazing technology. The drift tube shape can be optimized to reduce capacitance and peak power density. To put quadrupole magnets inside the drift tubes would require a shallower face angle, which would result in more power dissipation on the drift tube. It also would require a method of assembly that would not damage the magnet material.
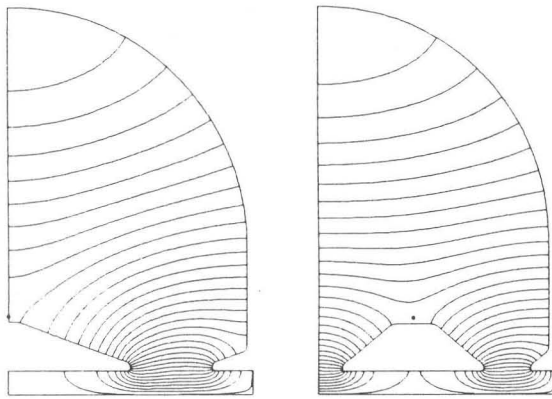

Figure 3. Two CCDTL half cavities. The bottom of each figure is the beam axis and the left-hand edge is a symmetry plane. The contours are SUPERFISH-calculated lines of constant rH. The one-drift-tube cavity at left is for β = 0.314 (50-MeV protons). The two-drift-tube cavity at right has the same length and is for β = 0.188 (17.1-MeV protons).

The CCDTL has a high efficiency in spite of its large wall surface compared to a DTL (see the next section). This efficiency is due in part to a large transit-time factor T. The electric field contours in Figure 3 illustrate why T is large in the CCDTL. The π-mode or Dirichlet boundary between accelerating cavities (right side of figures) results in a higher T than the 0-mode or Neumann boundaries between cells of a DTL. A CCDTL with one drift tube per cavity has an equal number of π-mode and 0-mode boundaries between cells. In the two-drift-tube cavity, a third of the boundaries are π-mode. The differences between 0-mode and π-mode boundaries are more pronounced for large-bore machines.

Shunt Impedance Calculations

For 2-D geometries with cylindrical symmetry, SUPERFISH calculates ZT^2, the effective shunt impedance per unit length. Figure 4 shows ZT^2 versus particle velocity for several 700-MHz cavities. The velocity range corresponds to proton energies between 5 and 200 MeV. Computer programs, called tuning codes (DTLFISH for DTL cells, CCLFISH for CCL cells, and CDTFISH for CCDTL cavities), adjust the cell geometry for resonance at a desired frequency. These codes run the SUPERFISH programs after each adjustment until the cavity is tuned within a specified tolerance. For this study, the code fixed the gap at βλ/4 and varied the cavity outer diameter to tune each cavity to 700±0.05 MHz. (For the longer cavities at higher β, this procedure results in a high peak power density. In practice, for the high-β cells of a high-duty linac, one would fix the diameter and tune by enlarging the gap.) The frequency of 700 MHz was the design frequency of a 7-cell bridge-coupled DTL (BCDTL) proposed in an early design for the Accelerator for Production of Tritium (APT) study.[3] We chose this structure for comparison with CCLs and CCDTLs because it also uses focusing magnets external to the rf structure. More recent designs for APT and other high-current linacs use a CCDTL instead of a BCDTL.
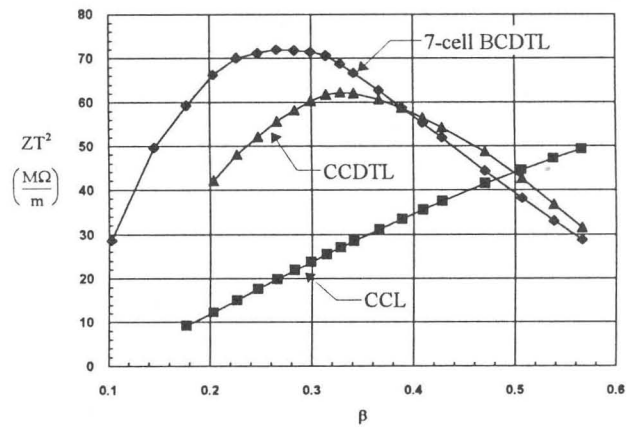

Figure 4. SUPERFISH ZT^2, the effective shunt impedance per unit length, versus particle velocity for the DTL, CCL and CCDTL structures.

The actual power losses for these structures are higher than shown in Figure 4, thus reducing the effective shunt impedance. For DTL tanks, the SUPERFISH value includes the power losses on stems and end walls, but not losses from rf joints, pumping holes, static or dynamic tuners, or post couplers. These additional losses typically add 25% to the SUPERFISH-calculated power. The coupling slot in CCL cavities increases power losses by about 3% for each percent of coupling. Because the CCL is a brazed structure, losses from rf joints are negligible. A typical CCL at 100 MeV has about 6% cell-to-cell coupling, so the CCL values will drop to about 82% of the SUPERFISH ZT^2. For a coupled-cavity structure the power-flow droop depends on the square of the number of

cavities divided by the square of the coupling constant. The droop is also inversely proportional to the coupling-cell Q times the accelerating-cell Q. The CCDTL cavity Q exceeds that of the CCL, especially at low β. This gives the CCDTL a lower power-flow droop for the same coupling and number of cavities. A CCDTL has one third the number of cavities per unit length as a CCL at the same β. Thus, even if the CCDTL and CCL had the same Q, 2% coupling in a one-drift-tube CCDTL provides the same field stability as 6% coupling provides in the CCL. For comparison to the other structures, the CCDTL needs only 2% coupling. Figure 5 shows ZT^2 versus β after correcting for the additional power losses. The BCDTL values have been multiplied by 0.80, CCL values by 0.82, and CCDTL values by 0.94.
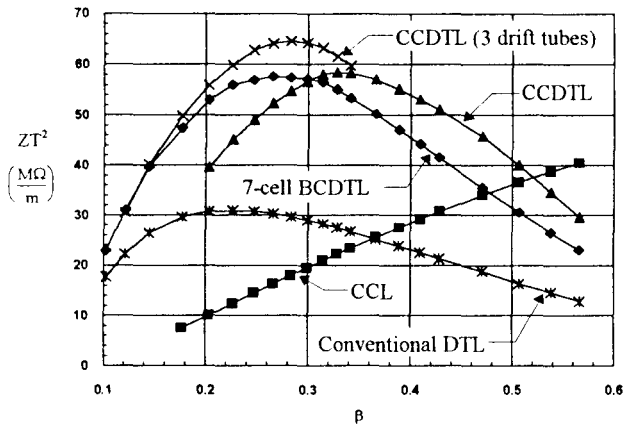

Figure 5. ZT^2 versus particle velocity from Figure 4 corrected for power losses not included by SUPERFISH. Also shown are curves for a CCDTL with 3 drift tubes per cavity and a conventional DTL with drift tubes large enough for focusing magnets.

The calculations for the CCL, CCDTL, and 7-cell BCDTL used the same nose shape and bore radius for all cavities. For a given β, the BCDTL and CCDTL had identical drift tubes. Using the same drift-tube shape allows a fair comparison between structures. Any linac design that used these structures would have similar transverse focusing requirements that could be provided with magnets external to the cavities. This "dead space" reduces ZT^2 by the ratio of active accelerator length to total length, but it affects all the designs in the same way. The 7-cell BCDTL is a highly optimized structure. For reference, Figure 5 includes a conventional DTL (also at 700 MHz) that has 8-cm-diameter drift tubes with a 10° face angle. Its entire length is active structure because the drift tubes hold quadrupole magnets. However, the nose shape increases capacitance and hence power losses. A frequency of 700 MHz may not be the best choice for a conventional DTL. For adequate room in the drift tubes for focusing, accelerator designs often start with a lower frequency DTL, which injects a CCL operating at a whole number multiple of the DTL frequency. For example, a 350-MHz DTL could inject a 700-MHz CCL.

Stability Considerations

Figure 5 includes a curve for a three-drift-tube CCDTL. Two- and three-drift-tube cavities become more advantageous than one-drift-tube cavities at low β. These structures have stability similar to a one-drift-tube CCDTL for higher β because the cavity length is short (less than λ for the operating mode). Figure 6 shows a two-drift-tube CCDTL. The accelerating cavity has the same length as a $\beta = 0.314$ cavity with one drift tube (see Figure 1). The two-drift-tube cavity length is $5\beta\lambda/2$, so this structure corresponds to $\beta = 0.188$. The calculated shunt-impedance curve for this structure lies between the two CCDTL curves in Figure 5 (for structures with either one or three drift tubes).
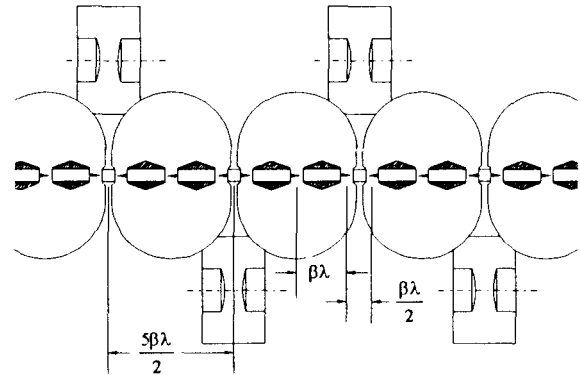

Figure 6. A two-drift-tube CCDTL structure for $\beta = 0.188$. The cavities are the same length as the cavities for $\beta = 0.314$ shown in Figure 1.

We numerically simulated two long structures: a CCDTL and a series of coupled 7-cell DTL tanks. For simplicity, we used 50-MeV cavities for each entire structure. With 5% coupling in the CCDTL (a typical and easily achieved value for short cavities), the power-flow droop at distance of $126\beta\lambda$ (84 accelerating cells) from the drive was about 3%. Coupling is proportional to H^2/U, where H is the magnetic field at the slot and U is the cavity stored energy. SUPERFISH runs indicated that H^2/U is 6.5 times lower in the DTL tanks, so 1% coupling will be hard to achieve. Nevertheless, if we assumed 1% coupling, the DTL had a 20% power-flow droop the same distance (19 tanks) from the drive. The power-flow phase shift from cell 1 to cell 7 in the first tank was 8°. The CCDTL had no such problems with power-flow phase shifts.

3-D Code Calculations

A 3-D study using MAFIA, Rel. 3.2 started with geometrical parameters from SUPERFISH for a $\beta = 0.283$ CCDTL at 1400 MHz. We switched from 700 to 1400 MHz structures because the higher frequency made the first low-power model a more manageable size. So far, we have studied only one-drift-tube CCDTL structures with the 3-D code. We first tuned the accelerating and coupling cavities separately and then assembled them into a coupled structure with stems

and coupling slots. The slots detune the main and coupling cavities differently, so the geometry that we initially modeled had a large stopband of 28 MHz for the TM_{010} mode spectrum. Figure 7 shows the 3-D mesh and electric field of the operating mode for a typical run.

We investigated modes introduced by one or two stems in a single CCDTL cavity without coupling slots. Post-coupled, multiple-stem DTLs can have stem-related modes near the accelerating mode.[4] The CCDTL has no post couplers (as in Ref. 4), so we hoped to confirm with the code that these modes would not pose a problem. Table 1 lists the MAFIA-calculated frequencies of the stem-related mode nearest the TM_{010} mode for stem angles from 0° (single stem) to 180° for the $\beta = 0.283$ structure. In this mode, the area between the stems is depleted of field for angles smaller than 180°. These frequencies far exceed the 1400-MHz frequency of the accelerating mode. Thus, at least for $\beta = 0.283$, this mode creates no problems. The mode frequencies vary smoothly and monotonically from one stem to two stems 180° apart. This means that we need calculations only for a single stem and for two stems 180° apart to find the range of frequencies in a cavity for another β. For example, at $\beta = 0.5$, the lower frequency bound is 1636 MHz (single stem) and the upper bound is 2159 MHz (180° between two stems). For cavities with $\beta < 0.283$, the modes are all well above 2000 MHz. Thus, for the useful energy range of the CCDTL, there is no problem from this kind of stem mode. More calculations of this type will be needed for CCDTL cavities containing two or three drift tubes.

Table 1. Nearest Stem-Related Modes for $\beta = 0.283$.

Stem Angle (degrees)	Frequency (MHz)
0	2055
60	2090
90	2132
120	2161
180	2207

Low-Power Model Measurements

We recently began testing a low-power aluminum model of a $\beta = 0.283$, 1400-MHz CCDTL structure. With this model we can measure the TM_{010} mode spectrum, from which it is possible to calculate the coupling between cells and the stopband. We can also investigate the effects of different stem configurations on the operating mode. Figure 8 shows the model assembled with one full accelerating cell, two coupling cells and half accelerating cells on the ends. The model incorporates some features that we intend to use in the construction of brazed copper structures. The ring holding the drift tube is the main difference between a conventional CCL and a CCDTL. In a two-stem configuration, coolant for the drift tube would flow in one stem and out the other. Web cooling between accelerating cells of a CCDTL would be virtually identical to a standard CCL.
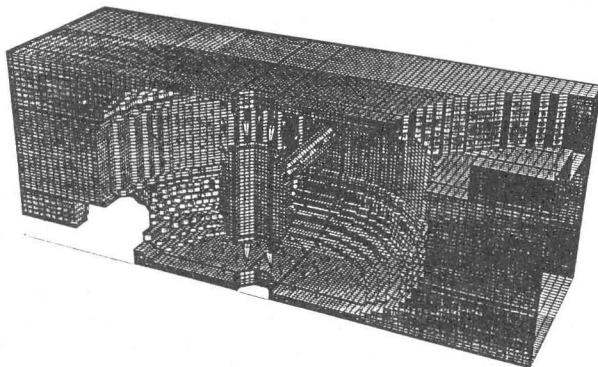

Figure 7. MAFIA-generated mesh and electric field for the 1400-MHz CCDTL operating mode. Though this plot shows only part of the coupling cell, the model included the full geometry of the coupling cells.

For further 3-D calculations, we must first better tune the cavities of the numerical model to reduce the stopband. Something we plan to investigate is the possible presence of dipole modes (with electric field normal to the beam axis) at twice the frequency of the operating mode. Appropriate choices for the cavity diameter and drift-tube gaps can tune these modes away from undesirable frequencies.
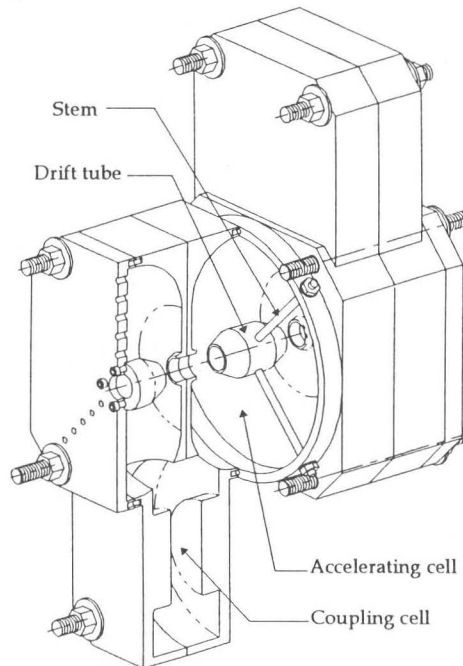

Figure 8. Cut-away view of the CCDTL low-power model. The parts can be assembled with either full or half cells of either accelerating cells or coupling cells on the ends. A separate ring holds the drift tube. This view shows two stems in one of many possible orientations.

We tested a 7-cell structure consisting of two full accelerating cavities, three coupling cells, and half accelerating cells on the ends. This structure was the same as the one in Figure 8 with one more full accelerating cell. Initial frequency measurements with one stem 90° from the coupling slots indicated a stopband of −12.3 MHz. Machining 0.23 mm from the coupling-cell noses raised the average frequency of the coupling cells and changed the stopband to +1.1 MHz. Table 2 lists the measured mode frequencies of the TM_{010} passband. Figure 9 shows a fitted dispersion curve for the single-stem data. The second stem raised the frequency of the full accelerating cells and reintroduced a negative stopband. We can, of course, retune the coupling cells to close the stopband, but we will first complete other single-stem tests. These measurements indicate that the coupling is about 2.7% between the accelerating cells and the coupling cells.

Table 2. Mode Frequencies in a 7-Cell Low-Power CCDTL

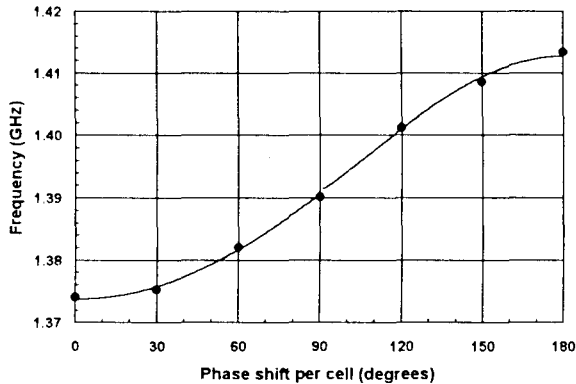| Mode	Single stem	Two stems
0	1373.98	1374.73
$\pi/6$	1375.26	1375.58
$\pi/3$	1382.03	1382.74
$\pi/2$	1390.16	1393.48
$2\pi/3$	1401.16	1401.21
$5\pi/6$	1408.52	1410.44
π	1413.31	1415.78

Figure 9. Dispersion curve fitted to the 7-cell CCDTL modes for a single stem. The stopband is +1.1 MHz and the first-neighbor coupling is 2.7%.

Figure 10 shows the relative field strength on the axis in the $\pi/2$ mode of the 7-cell model. An automated measurement system recorded changes in resonant frequency as a 0.5-mm-diameter bead traversed the cavity at constant speed.[5] The largest frequency shift observed was about 120 kHz. The relative field shown in the figure is proportional to the square root of the observed frequency shift. The field actually reverses direction between peaks 1 and 2, peaks 3 and 4, and peaks 5 and 6. However, the measurement is sensitive only to the square of the field, so all the data appear as positive values. The first and last peaks correspond to the field in the gap of

the end half cells. The second and third peaks are in the first full accelerating cell and the fourth and fifth peaks are in the second full cell. Later, we will reduce the few-percent variation in the field amplitudes by trimming the size of some of the coupling slots.
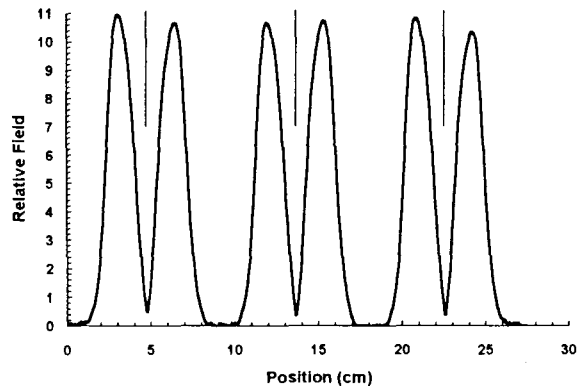
Figure 10. Results of an axial bead-perturbation measurement for the $\pi/2$ mode of the 7-cell CCDTL model. Vertical lines show the boundaries between accelerating cavities.

Conclusions

The CCDTL structure has a better shunt impedance than either the DTL or CCL structures over a wide range of β. It competes favorably with the DTL at low β if one uses more than one drift tube per accelerating cavity. Even the one-drift-tube version at $\beta = 0.2$ (20-MeV protons) has a higher ZT^2 than a conventional CCL has at $\beta = 0.42$ (100-MeV protons). Field stability in the CCDTL is good because the individual cavities are always shorter than a single wavelength of the operating mode.

References

1 E. A. Knapp, P. W. Allison, C. R. Emigh, L. N. Engel, J. M. Potter, and W. J. Shlaer, "Accelerating Structure Research at Los Alamos," Proceedings of the 1966 Linear Accelerator Conference, Los Alamos National Laboratory Report LA-3609, p. 83 (1966).

2 J. M. Watson, "The SSC Linac,", Proceedings of the 1990 Linear Accelerator Conference, Los Alamos National Laboratory Report LA-12004C, p. 31 (1991).

3 Los Alamos National Laboratory APT Topical Report, LA-12668-MS (September, 1993).

4 J. H. Billen, G. Spalek, and A. H. Shapiro, "Field Stability in Two-Stem Drift-Tube Linacs," Proceedings of the 1988 Linear Accelerator Conference, CEBAF Report 89-001, p. 125 (1989).

5 J. H. Billen, "Radio Frequency Measurement and Analysis Codes," Proceedings of the 1993 Particle Accelerator Conference, Vol. 2, p. 793 (1993).